

Modelling of a lens system for the optical beam focusing of diode laser bars with high fill factor for optoacoustic applications

Luca LEGGIO*, Bartosz WIŚNIEWSKI, Sandeep Babu GAWALI, Daniel GALLEGRO, Miguel SÁNCHEZ, Sergio RODRÍGUEZ, Guillermo CARPINTERO, and Horacio LAMELA

Department of Electronics Technology, Optoelectronic and Laser Technology Group (GOTL), University Carlos III of Madrid, Av. de la Universidad, 30, 28911, Leganés (Spain) (lleggio@ing.uc3m.es)

Abstract

A customized optical system composed of collimating and focusing lenses is proposed to achieve the beam focusing of high-brightness diode laser bars with high fill factor for optoacoustic applications. Through an optimized design, the beam of a 940-nm diode laser bar is first collimated and symmetrized between the fast and slow axes, and then is reduced in size into a square beam ($\sim 3.7 \text{ mm} \times 3.7 \text{ mm}$ at $1/e^2$ of the peak) with intensity of $\sim 3.2 \text{ kW/cm}^2$. In an optoacoustic environment, the optical spot achieved can illuminate a small region of tissue at high intensity to achieve in-depth imaging with high resolution.

Keywords: Diode laser bars, Laser beam shaping, Microlenses, Optoacoustics.

1. Introduction

High-power diode laser bars (DLBs) and stacks (DLSs) are extensively used in several applications, such as metal welding and soldering [1], surface treatments [2], solar cells fabrication [3], laser surgery [4], molecular and atomic spectroscopy, and military defense [5]. Recently, DLSs at 808 nm have been proposed also for optoacoustic applications [6]. These devices can provide very high values of optical peak power (from hundreds of W to several kW), but they suffer from high divergence of the propagated beam [2] that requires additional optical elements for beam shaping [7]. Industrial applications already have solutions for beam shaping of DLBs and DLSs with fill factor up to 50 % (the fill factor is the ratio between the emitter width and the emitter pitch and is expressed in percentile). Their brightness increases with the fill factor, but their beam gets more complex to handle due to the short distance between emitters. Unfortunately, the market does not offer appropriate lenses to collimate the beam of diode laser devices with fill factor greater than 50 %. In this case the beam collimation is problematic because the array of

slow axis collimation (SAC) lenses should be very close to the source, due to the short distance between adjacent emitters that causes a “fast” divergence of the slow axis in short distances. Consequently, there would be not space to include a fast axis collimation (FAC) lens that normally comes first [8-9]. In this paper, the technical goal is to develop a laser source to illuminate a target at high intensity with a near-square pattern. The approach is to use a high-power DLB with fill factor of 76 % (emitter width and pitch of 190 μm and 250 μm , respectively), taking into account a realistic model of Jenoptik (JDL-BAB-75-37-940-TE-300-1.5) with 37 emitters and radiating in the near-infrared (NIR) at the central wavelength of 940 nm, suitable for optoacoustic imaging [10]. We propose a customized lens design for this DLB. Collimating and beam focusing lenses have been designed in Zemax environment to reduce the beam size of the abovementioned DLB. In this case, the collimating lenses have not been positioned close to the source but at a certain distance that allows the beam symmetrization between the two axes and the

collimation. More specifically, cylindrical FAC and SAC lenses have been positioned at 12 mm and 23 mm from the DLB, respectively. In such a way, the beam is symmetrized and collimated at the same time. As a result, the beam observed on a detector plane (at 40 mm from the source) shows a semi-square shape ($\sim 12.35 \text{ mm} \times 11.62 \text{ mm}$) that facilitates its handling in a successive stage. Then, a second pair of crossed cylindrical lenses has been designed to reduce the beam size. Successively, another pair of cylindrical lenses (one plano-concave and the other one plano-convex) is used to reshape the beam in a smaller spot with size of $\sim 3.7 \text{ mm} \times 3.7 \text{ mm}$ (at $1/e^2$) and intensity of $\sim 3.2 \text{ kW/cm}^2$. Due to the large number of emitters, the beam spot could not be reduced more in the slow axis. Basically, the

latter lens pair has been designed to achieve a square spot for optoacoustic applications in which a homogeneous beam profile is required for uniform light focusing on an absorbing target.

2. Results

The beam collimation is showed in Figure 1 and the optical elements are arranged following the order of the abovementioned description. In Table 1, the main characteristics of the DLB are reported. The high number of emitters (37) of this bar is responsible for such high output peak power (300 W) but goes to the detriment of the beam quality, due to a higher beam parameter product (*BPP*). The characteristics of the collimating lenses are listed in Table 2.

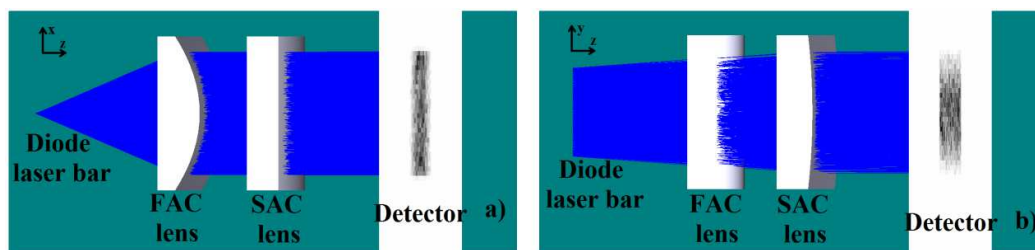


Figure 1. Simulation scheme of the optical system collimating a DLB from Jenoptik (JDL-BAB-75-37-940-TE-300-1.5) with 37 emitters and 76 % fill factor: lateral view of a) fast axis and b) slow axis. The emitter width and pitch are $190 \mu\text{m}$ and $250 \mu\text{m}$, respectively. The image shows very good collimation in both axes. Actually, the beam is not collimated but keeps a semi-square pattern for a certain distance after the SAC lens (i.e. $\sim 88 \text{ mm}$).

Table 1. Main characteristics of the DLB. *Quasi-continuous wave

Characteristic	Value
Central wavelength	940 nm
Regime	QCW*
Output peak power	300 W
Fast axis beam divergence ($1/e^2$)	$47.5 \pm 1.5^\circ$
Slow axis beam divergence ($1/e^2$)	$10 \pm 1^\circ$
Single emitter contact width	$190 \mu\text{m}$
Emitter pitch	$250 \mu\text{m}$
Number of emitters	37
Fill factor	76%

The beam-parameter product (BPP) is necessary to estimate the beam quality in both fast and slow axes. In fast axis, it is defined as the waist radius w_{0x} (i.e. the half of the vertical size in fast axis) multiplied by the half angle divergence $\theta_{\perp half}$ of the beam along the fast axis. Instead, in the slow axis it corresponds to the waist radius w_{0y} (which in our case corresponds to the half of the emitter width in slow axis (see Table 1)) multiplied by the half angle divergence $\theta_{//half}$ of the beam along the slow axis and the number of emitters, normalized to the bar fill factor. Hence, the BPP_s in fast axis (BPP_x) and slow axis (BPP_y) are respectively expressed by:

$$BPP_x = w_{0x} \times \theta_{\perp half} \quad (1)$$

$$BPP_y = \frac{w_{0y} \times \theta_{//half} \times \text{number of emitters}}{\text{bar fill factor}} \quad (2)$$

where the bar fill factor is normally expressed in % and is the ratio between the emitter width and the emitter pitch (Table 1). In order to achieve the

necessary beam quality for an efficient fiber coupling, the BPP ratio (BPP_y/BPP_x) should be made as close as possible to 1 by means of beam shaping lenses. Assuming a vertical size of $2 \mu\text{m}$ (namely $w_{0x} = 1 \mu\text{m}$) for each emitter, at the output of the DLB, the BPP_s in fast axis (BPP_x) and slow axis (BPP_y) are respectively:

$$BPP_x = 1 \mu\text{m} \times 23.75^\circ \approx 0.41 \mu\text{m} \cdot \text{rad}, \quad (3)$$

$$BPP_y = \frac{95 \mu\text{m} \times 5^\circ \times 37 \text{ emitters}}{\text{fill factor}} \approx 403.607 \mu\text{m} \cdot \text{rad}, \quad (4)$$

Hence, from Eqs. (3) and (4) it can be derived that:

$$\frac{BPP_y}{BPP_x} \approx 984.4 \quad (5)$$

that will be significantly reduced after collimation. Figure 2 shows more in detail the DLB composed of an array of emitters.

Table 2. Characteristics of the collimating lenses.

Component	FAC lens	SAC lens
Material	N-LAF21	N-LAF21
Height (mm)	16	16
Thickness (mm)	4.5	3.8
Length (mm)	16	16
Radii of curvature (mm)	Infinite/ 11.1	Infinite/ 70
Conic constant	-1	-1
Distance from DLB (mm)	12	23

It can be noticed how much is short the spacing between adjacent emitters. Even though the slow axis divergence is little ($10 \pm 1^\circ$), the rays of each emitter intersect those of the adjacent emitters at very close distances from the source. The beam profile simulated at 40 mm from the source is represented in Figs. 3 and 4 as graph and image,

respectively. Both the FAC and SAC lenses are plano-convex and their curvature is in the front face of the lenses. As a result, the collimated beam takes a semi-square shape ($\sim 12.35 \text{ mm} \times 11.62 \text{ mm}$ at $1/e^2$ of the peak) that is easier to focus in a successive stage. The detector image shows that the major contribution of power is in the central part of the

beam, following the principle of Gaussian beam. In a second step we show the beam focusing in a square spot. Normally, in optoacoustic applications is required to focus the beam in a spot to illuminate small regions of biological tissues for in-depth imaging with high resolution. In this regard, we reduced the beam size in a square spot of $\sim 3.7 \text{ mm} \times 3.7 \text{ mm}$ (at $1/e^2$) using two additional pairs of cylindrical lenses. The characteristics of these lenses are listed in Table 3 and they are labeled with their numeration. Figure 5 shows the whole lens system including the focusing lenses to reduce the beam spot size. The square spot is captured at a distance of 75 mm from the source (Figure 6). The spot size is a square with size of $\sim 3.7 \text{ mm} \times 3.7 \text{ mm}$ and intensity of $\sim 3.2 \text{ kW/cm}^2$ (Figs. 6 and 7). At this stage, the values for the two BPP_s have now been nearly symmetrized. The BPP_y has been reduced to $403.607 \mu\text{m}\cdot\text{rad} / 37 \approx 10.908 \mu\text{m}\cdot\text{rad}$, while BPP_x has increased to $0.41 \mu\text{m}\cdot\text{rad} \times 37 \approx 15.17 \mu\text{m}\cdot\text{rad}$. In such a way, it can be derived that:

$$\frac{BPP_x}{BPP_y} \approx 1.39 \quad (6)$$

which corresponds to a BPP reduction factor of ~ 708 . Then, the footprint on the target is reduced by a linear factor of ~ 37 , and the intensity on target is increased by a factor of $\sim 37^2 = 1369$. The intensity on the detector is limited by the inability to reduce the square footprint below 37 mm in the slow axis. This depends directly on the large value of BPP_y at the output of the DLB. Considering a typical pulse width of 200 ns in optoacoustic applications [11], the intensity of $\sim 3.2 \text{ kW/cm}^2$ achieved with the proposed design corresponds to 0.64 mJ/cm^2 , which is compatible with the limit of maximum energy density applicable to a biological tissue, which is 20 mJ/cm^2 following ANSI safety standard. The large number of the emitters, combined with the high fill factor of this DLB, does not allow the beam focusing in a smaller spot that is required in optoacoustic endoscopy using coupling into optical fibers ($< 600 \mu\text{m}$), but consents other optoacoustic applications in free space.

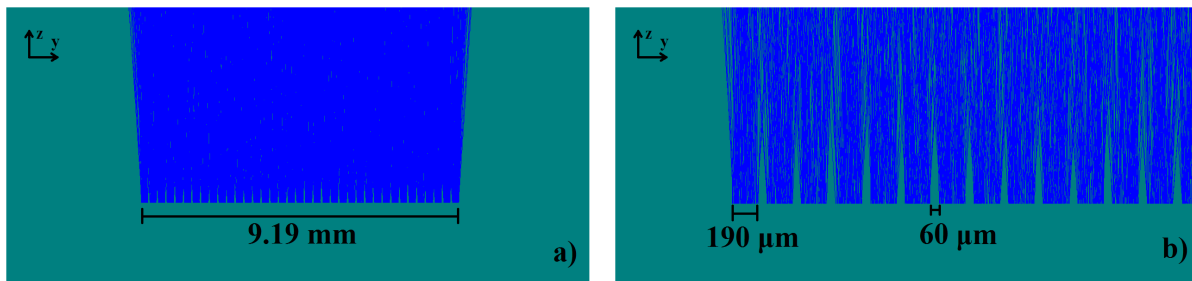


Figure 2. DLB array of 37 emitters at close distance: a) size of the whole array, b) size of each emitter and pitch.

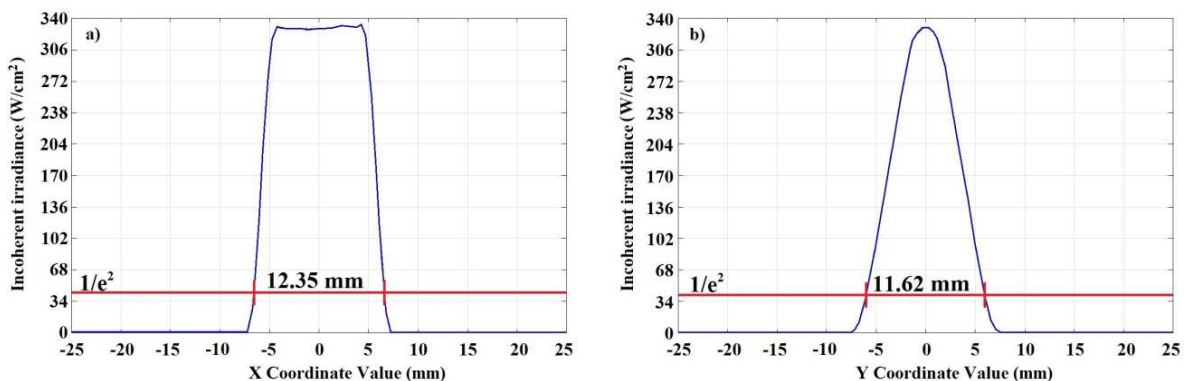


Figure 3. Profile of the collimated beam in: a) fast axis and b) slow axis. The beam size is $\sim 12.35 \text{ mm} \times 11.62 \text{ mm}$ at $1/e^2$.

Luca LEGGIO, Bartosz WIŚNIEWSKI, Sandeep B. GAWALI, Miguel SÁNCHEZ, Sergio RODRÍGUEZ, *et al.*
Modelling of a lens system for the optical beam focusing of diode laser bars with high fill factor

Detector image of collimated beam (W/cm²)

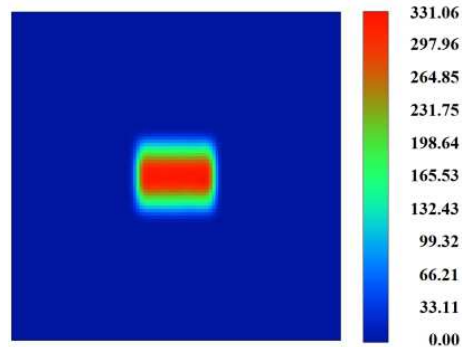


Figure 4. Image of the beam profile observed on a detector located after collimating lenses.

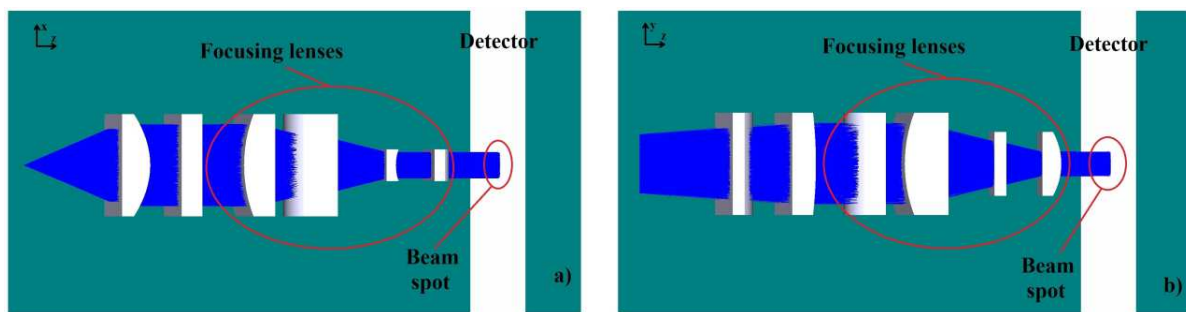


Figure 5. Whole lens system to reduce the size of the beam spot: a) lateral view, b) top view. At longer distances (i.e. ~ 8 mm from the last focusing lens), the beam divergence would be larger in the slow axis due to the large number of emitters.

Table 3. Characteristics of each focusing lens for beam size reduction.

Component	Focusing lens 1	Focusing lens 2	Focusing lens 3	Focusing lens 4
Material	S-LAH64	S-LAH64	S-TIH53	S-TIH53
Height (mm)	16	16	5	5
Thickness (mm)	5	7	1.5	3
Length (mm)	16	16	10	10
Radii of curvature (mm)	-21.984/ Infinite	-21.984/ Infinite	Infinite/ -7.5	Infinite/ 10
Conic constant	0	0	0	0
Distance from DLB (mm)	33	41	56.3	64

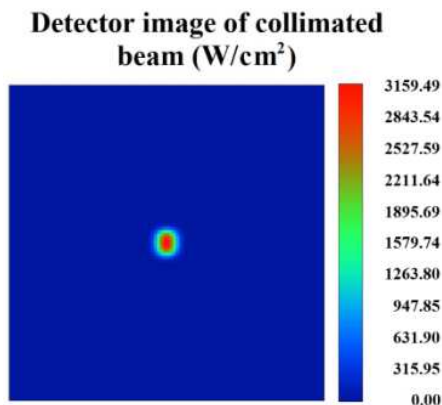


Figure 6. Image of the beam focused observed on a detector.

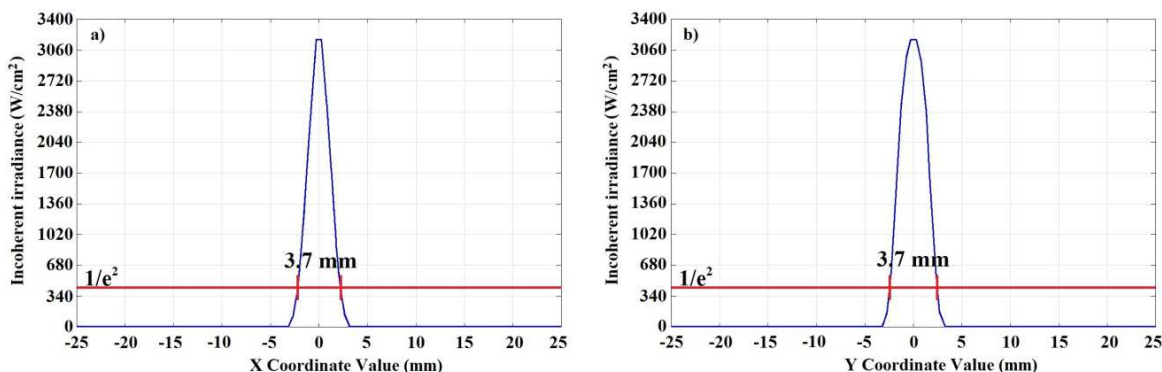


Figure 7. Beam profile of the focused beam in: a) fast axis and b) slow axis. The beam size is $\sim 3.7 \times 3.7$ mm at $1/e^2$.

Conclusions

In summary, we have presented the design of a customized lens system to reduce the beam size of DLBs with fill factor greater than 50 %. Our results demonstrate a good collimation in both fast and slow axis and a focusing in a small spot. This work opens the opportunity of development of the proposed lenses for beam focusing of DLBs with high fill factor. Their characteristics of high brilliance and high optical power are particularly useful for penetrating in depth into biological tissues. Future work should be addressed to the implementation of the lens system proposed in this paper.

In this way, the optoacoustic imaging at 940 nm of some chromophores like lipids and hemoglobin would get benefit from these DLBs.

Acknowledgment

Our work is supported by EU research project OILTEBIA (Optical Imaging and Laser TEchniques for Blomedical Applications).

Declaration of interest

The authors have no financial interests in the manuscript. There are no potential conflicts of interest to declare.



References

- [1] Sanchez-Rubio A., Fan T.Y., Augst S.J., Goyal A.K., Creedon K.J., *et al.* Wavelength beam combining for power and brightness scaling of laser systems. *Lincoln Laboratory Journal* 2014; 20 (2): 52-66.
- [2] Bachmann F., Loosen P., and Poprawe, R. High power diode lasers: technology and applications. Springer Science Eds., ISBN 978-0-387-34729-5 Berlin, Germany; 2007.
- [3] Lichtenstein N., Baettig R., Brunner R., Müller J., Valk B., *et al.* Scalable, high power line focus diode laser for crystallizing of silicon thin films. *Physics Procedia* 2010; 5 (Part A): 109-117.
- [4] Webb C. and Jones J. Handbook of laser technology and applications: laser design and laser systems. ISBN 9780750306072, Vol. 2, CRC Press; 2004.
- [5] McAulay A.D. Military laser technology for defense: technology for revolutionizing 21st century warfare. John Wiley & Sons, Inc., Hoboken, U.S.A. 2011, ISBN: 978-0-470-25560-5.
- [6] Sánchez M., Rodríguez S., Leggio L., Gawali S., Gallego D., *et al.* Beam profile improvement of a high-power diode laser stack for optoacoustic applications. *International Journal of Thermophysics* 2017; 38 (48).
- [7] Sturm V., Treusch H.G., and Loosen P. Cylindrical microlenses for collimating high-power diode lasers. *Lasers in Material Processing, Proc. of SPIE* 1997; 3097: 717-726.
- [8] Leggio L., Gallego D.C., Gawali S.B., Sánchez M., Rodríguez S., *et al.* System analysis of wavelength-beam combining of high-power diode lasers for photoacoustic endoscopy. *Proc. of SPIE* 2016; 9888.
- [9] Yu J., Guo L., Wu H., Wang Z., Gao S., *et al.* Optimization of beam transformation system for laser-diode bars. *Optics Express* 2016; 24 (17): 19728-35.
- [10] Fehm T.F., Deán-Ben X.L., Schaur P., Sroka R., and Razansky D. Volumetric optoacoustic imaging feedback during endovenous laser therapy – an ex vivo investigation. *Journal of Biophotonics* 2016; 9 (9): 934–941.
- [11] Allen T.J. and Beard P.C. Dual wavelength laser diode excitation source for 2D photoacoustic imaging. *Proc. of SPIE* 2007; 6437.